Int Ophthalmol (2026) 46:128
https://doi.org/10.1007/s10792-026-03946-7

ORIGINAL PAPER

Evaluation of hyperreflective spots as a novel biomarker in patients with glaucoma

Kıvanc Kasal · Yurdagul Girgin · Eyyup Karahan

Received: 25 October 2025 / Accepted: 18 January 2026

Abstract

Purpose To evaluate hyperreflective spots (HRS) detected by optical coherence tomography (OCT) in healthy and glaucomatous eyes and their correlation with retinal ganglion cell (RGC) loss.

Methods A total of 65 patients with primary open-angle glaucoma (POAG) and 65 healthy controls were enrolled, and data were collected from one eye of each participant. In glaucoma patients, the eye with better visual acuity was selected; if equal, the eye with the higher OCT image quality was included. In the control group, the eye with the higher OCT image quality was selected for analysis. OCT scans of the fovea's thinnest section were analyzed, and an area 3000 µm wide at the center was selected. HRS were defined as small spots (≤ 30 µm) with moderate reflectivity and no shadowing. HRS counts were compared between groups, and correlations with OCT parameters associated with RGC loss were assessed.

Results The mean age was similar between groups (glaucoma: 62.48 ± 19.77 years; control: 59.75 ± 6.65 years; $P = 0.085$). Inter-rater agreement for HRS counts was excellent (ICC = 0.927, 95% CI: 0.89–0.94). Glaucoma patients had significantly higher HRS counts than controls (29.65 ± 7.68 vs. 11.86 ± 5.05, $P < 0.001$). HRS counts positively correlated with vertical and horizontal cupping diameters ($r = 0.45$, $P < 0.001$) and negatively correlated with neuroretinal rim area ($r = -0.46$, $P < 0.001$), total RNFL thickness ($r = -0.39$, $P < 0.001$), and mean GCC thickness ($r = -0.43$, $P < 0.001$). Correlation coefficients were similar after adjusting for age, intraocular pressure (IOP), and signal strength index (SSI).

Conclusions HRS strongly correlate with RGC and RNFL loss in glaucoma and may serve as as a valuable biomarker in the follow-up of glaucoma.

Keywords Glaucoma · Hyper-reflective spot · Microglia cell · Neuroinflammation · Optical coherence tomography

Introduction

Glaucoma is a insidious progressive neurodegenerative disease that is one of the leading causes of irreversible severe vision loss. The loss of retinal ganglion cell (RGC) is characterized by thinning of the retinal nerve fiber layer (RNFL) and increased cupping of the optic disc. Elevated intraocular pressure (IOP), increasing age, and positive family

Yurdagül Girgin is presently affiliated with Tekirdağ Çorlu State Hospital.

K. Kasal (✉)
Department of Ophthalmology, Bigadic State Hospital, Balikesir, Turkey
e-mail: kvnckasal90@gmail.com

Y. Girgin · E. Karahan
Department of Ophthalmology, Balıkesir University, Balikesir, Turkey

Published online: 24 February 2026

history are the most common risk factors for glaucoma [1]. Although IOP, the only modifiable risk factor, can be controlled through medical or surgical treatment, many glaucoma patients continue to progress [2]. In normotensive glaucoma, glaucomatous damage can be observed at the optic nerve head despite the IOP being within the normal range. This would imply that IOP is not the sole guilty factor in causing glaucomatous damage and further factors might also be involved in the process of progressing glaucomatous neurodegeneration leading to RGC death.

Mechanisms underlying the development of neurodegeneration include hypoxia/ischemia, mitochondrial dysfunction, oxidative stress, and neuroinflammation [3]. The interactions between microglial and macroglial cells (Müller cells and astrocytes) are important in the development of the inflammatory process. Glial cells play active roles in triggering and sustaining apoptosis in glaucoma [4]. Under physiological conditions, these cells maintain a delicate balance in the retina by providing nutrients and structural support to neurons. Through the release of neurotrophic factors and the phagocytosis of debris, they help to isolate neural tissue damage and subsequently promote neuroregeneration [5]. However, when the stress stimulus in the retina becomes chronic, inflammation can turn detrimental. The activation of microglial cells causes to the release of pro-inflammatory cytokines, complement components, and nitric oxide, contributing to inflammation [6, 7]. Microglial cells shorten, their bodies expand, they become amoeboid, mobilize, and proliferate. They then migrate towards the site of damaged tissue, leading to RGC loss. More than half of the RGCs in the entire retina are located in the macular region [8]. Therefore, neuroinflammation directed by microglial cells is observed in the inner layers of the macula, which consists of the inner plexiform layer, ganglion cell layer and RNFL, where the dendrites, soma and axons of RGCs are located, respectively.

In recent years, reactive microglial cells have been considered to be associated with hyperreflective spots (HRS) identified in macular sections obtained with optical coherence tomography (OCT) [9]. HRS are particularly noted in retinal diseases such as diabetic retinopathy and age-related macular degeneration, where inflammation is intense, as well as in multiple sclerosis, a neurodegenerative disease affecting the central nervous system [10–12]. Numerous studies have reported that HRS can serve as an OCT biomarker for assessing the severity of inflammation during the disease course and treatment response.

OCT is frequently used in the diagnosis and follow-up of glaucoma due to its non-invasive, repeatable nature and its ability to provide qualitative objective data. Assessment of glaucomatous damage is conducted based on parameters of the optic nerve head (C/D ratio, cup volume, neuroretinal rim thickness), RNFL thickness, and ganglion cell complex (GCC) thickness (RNFL, ganglion cell layer, and inner plexiform layer). A review of the literature reveals an increasing emphasis on the importance of neuroinflammation in glaucoma; however, only a limited number of studies have investigated the role of HRS as a potential biomarker. In an OCT-based study, HRS counts were significantly higher in glaucoma patients compared to healthy controls, and this increase was reported to be directly correlated with visual field loss [13]. In an experimental animal study, small hyperreflective opacities at vitreoretinal area were proposed as indicators of early homeostatic disruption in glaucoma, potentially involving microglia and macrophages [14].

The purpose of this study is to investigate whether HRS counts differ in glaucoma patients and to assess their potential as a novel biomarker for the monitoring of glaucomatous damage characterized by RGC loss.

Materials and methods

Sample selection

This observational study was carried out at the Ophthalmology Clinic of Balıkesir University Training and Research Hospital between April 2024 and September 2024. The study was conducted in accordance with the principles of the Helsinki Declaration. Approval was granted by the Balıkesir University Health Sciences Non-Interventional Research Ethics Committee (No: 2024/238). Informed consent was obtained from all patients regarding participation in the study and publication of the results.

The study group consisted of 65 eyes diagnosed with POAG, while the control group included 65 eyes of 65 healthy individuals who presented for routine

examination. POAG was defined as having an IOP above 21 mm Hg, the presence of abnormal optic disc characteristics (focal or diffuse thinning of the neuroretinal rim), an open iridocorneal angle assessed indirectly (ACA grading system) (van Herick III-IV), and the absence of any underlying conditions.

Inclusion criteria were: 30 years or older in age, diagnosed with POAG. The control group consisted of healthy individuals aged 30 and above without known systemic diseases and with normal findings in ophthalmological examination. Refractive errors in the participants were limited to less than ± 2 diopters in cylindrical measurements and ± 4 diopters in spherical measurements. In glaucoma patients, the eye selection was based on the visual acuity, and the better eye was included in the study. If the visual acuity was equal, the image quality of the OCT scan was considered, and the eye with the higher SSI (a value automatically given by device) was included. In the control group, the eye demonstrating a SSI on OCT imaging was selected for inclusion in the study.

Exclusion criteria included: History of systemic diseases such as diabetes mellitus, uncontrolled hypertension, autoimmune diseases; presence of accompanying retinal diseases (retinal vascular occlusion, macular degeneration, etc.); history of uveitis; previous glaucoma or retinal surgeries; and cataract surgery performed within the last 12 months. To ensure a quality assessment, individuals with a SSI below 50 in OCT examinations were excluded.

Interventions

All participants underwent a comprehensive ophthalmological examination. This examination included best-corrected visual acuity measurement, IOP measurement using a pneumotonometer, assessment of the iridocorneal angle using the van Herick method, and fundus examination using a 90-diopter non-contact slit-lamp lens.

The macula, optic nerve head (ONH), RNFL, and GCC were evaluated using SD-optical coherence tomography (RTVue XR Avanti scanner, Optovue Inc., Fremont, CA, USA). Macular examination was conducted in raster mode, obtaining 21 horizontal sections over a 12 × 4 mm area. The ONH examination included 12 radial scans measuring 3.4 mm in length and 6 concentric ring scans with a diameter between 2.5 and 4 mm, with the retina pigment epithelium and optic nerve edge being automatically detected by the software. Parameters analyzed included cup/disc area ratio, vertical cup/disc ratio, horizontal cup/disc ratio, disc area (mm^2), neuroretinal rim area (mm^2), and cup volume (mm^3). The thickness of the peripapillary RNFL (µm) was automatically calculated and analyzed separately for total (RNFL-Total) and sectoral (superior, RNFL-S; nasal, RNFL-N; inferior, RNFL-I; temporal, RNFL-T) measurements. The GCC scanning pattern was centered 0.75 mm temporally from the fovea, covering a 7 × 7 mm square grid area with 15 B-scans spaced 0.5 mm apart. GCC thickness included the RNFL, ganglion cell layer (GCL), and inner plexiform layer (IPL). Average GCC (µm), superior GCC (µm), and inferior GCC (µm) thickness were measured, and focal loss volume (FLV%) and global loss volume (GLV%) were calculated using the software. Pachymetric measurements were conducted using SD-OCT to determine central corneal thickness (µm).

HRS counting

Horizontal macular OCT images obtained from all participants were evaluated, and the section with the thinnest foveal thickness was selected and transferred as a '.tiff image' to ImageJ software (http://imagej.nih.gov/ij/; provided in the public domain by the National Institutes of Health, Bethesda, MD, USA). A region of interest (ROI) measuring 3000 × 1500 µm was defined, centered on the central foveola. HRS were counted separately by two independent masked researchers within the developed ROI for each image. Isolated, punctiform spots measuring ≤ 30 µm, with moderate reflectivity and no black shading between them (similar to RNFL), were defined as HRS. HRS counting was performed between the retinal layers remaining between the RNFL and the outer plexiform layer (Fig. 1).

Statistical analysis

All statistical analyses were performed using statistical software (SPSS Statistics v 27.0; IBM Corp., New York, NY, USA). Continuous variables were described as mean and standard deviation and tested for normality using the Kolmogorov–Smirnov test. Categorical variables were tested with the Chi-square test and reported as frequency and percentage.

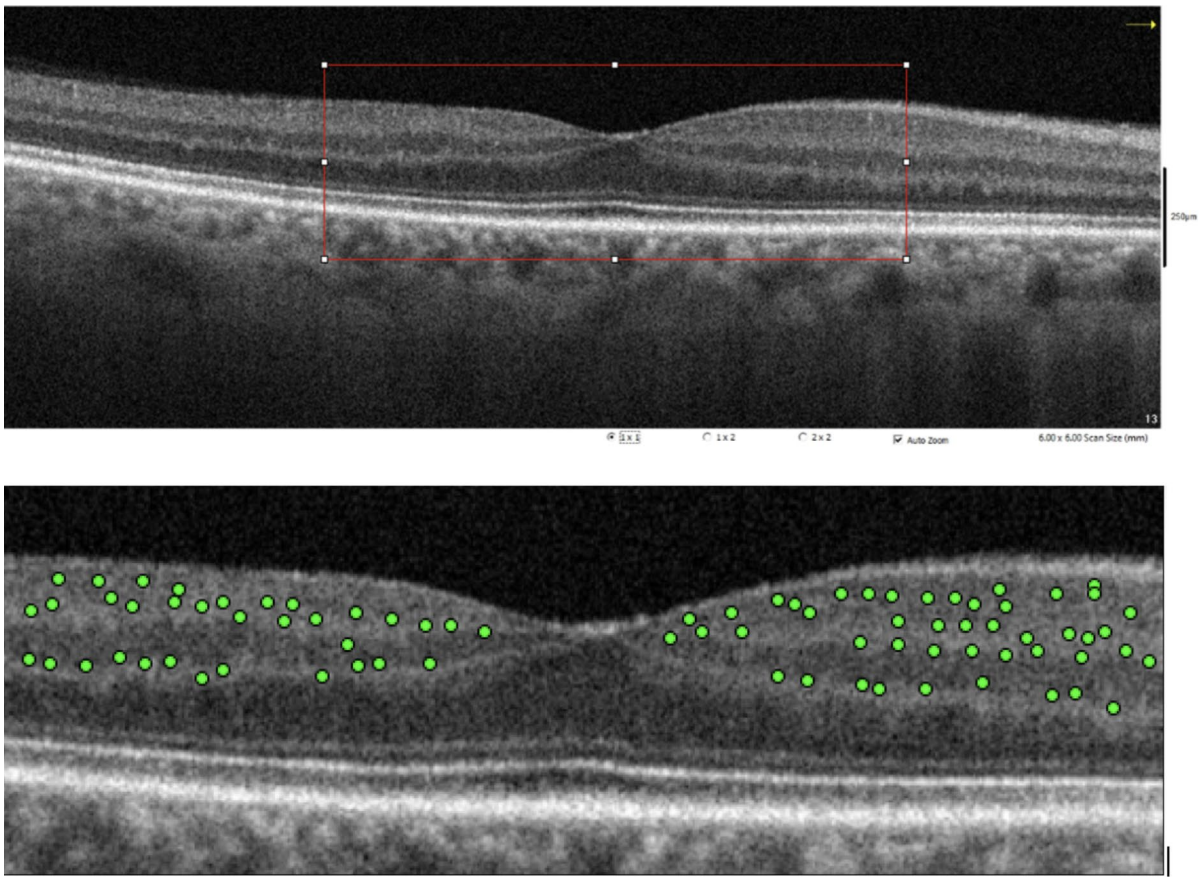

Fig. 1 Processing of OCT section using Image J software. After selecting the horizontal macular OCT section where the fovea is thinnest, a rectangular area with a center point on the foveola, a length of 1500 µm nasally and temporally, and a height that included all retinal layers was determined. (top). HRSs were marked by two researchers within the area as green dots (bottom). Abbreviations: OCT: Optic coherence tomography. HRS: Hyperreflective spots

Inter-rater and intra-rater reliability was evaluated using the intraclass correlation coefficient (ICC). A two-way ICC model was employed for all analyses. An ICC value of less than 0.50 was considered weak reliability, between 0.50 and 0.75 was moderate, between 0.75 and 0.90 was good and above 0.90 was considered excellent reliability.

The comparison of the number of HRS detected in glaucomatous and healthy individuals was performed using an independent-samples t-test. The p-value was assessed based on Levene's test for equality of variances. A significance level (p) of less than 0.05 was considered statistically significant. The correlation between the presence of glaucoma and the number of HRS (the average of the two researchers' HRS counts) and the correlation between the number of HRS and the ONH, RNFL thickness, and GCC parameters were evaluated using Spearman correlation tests. A partial correlation coefficient controlling for age, IOP and SSI was used to evaluate the linear correlation between the number of HRS and OCT parameters. Correlation coefficients (r) were interpreted as follows: 0.10–0.29 as low, 0.30–0.49 as moderate, and 0.50–1.00 as high correlation.

Results

A total of 65 eyes from patients diagnosed with POAG and 65 eyes from healthy individuals met the inclusion criteria and were included in the study. The average age was 62.48 ± 19.77 in the POAG group

and 59.75 ± 6.65 for the control group, ($P = 0.085$). In the glaucoma group, the proportion of women was 27/65 (41.5%); in the control group, it was 32/65 (49.2%). No significant differences were found between both group in terms of gender ($P = 0.378$). No significant differences were observed between the two groups regarding intraocular pressure and central corneal thickness ($P = 0.61$ and $P = 0.43$). However, best-corrected visual acuity was significantly lower in the glaucoma group ($P < 0.001$). The mean duration of follow-up for patients with POAG at the time of OCT imaging was 46.37 ± 52.92 months (Table 1). In the glaucoma group, no patient had a history of laser or surgical treatment. All patients were using at least one topical antiglaucomatous agent.

The horizontal and vertical cup-to-disc (C/D) ratios, neuroretinal rim area, and cup volume values showed significant differences between the two groups. Both C/D ratios and cup volume were found to be higher in the glaucoma group compared to the control group, while the neuroretinal rim area was significantly lower in individuals with glaucoma. No statistically significant difference was observed between the groups regarding optic disc area. Individuals with glaucoma had significantly thinner RNFL measurements in all quadrants (superior, temporal, inferior, and nasal) as well as in total. Similarly, the mean GCC thickness was found to be thinner in the study group compared to the healthy group (Fig. 2).

Regarding the counting of HRS, the inter-rater reliability level was found to be excellent according to the two-way intraclass correlation coefficient (ICC) analysis (ICC = 0.927, 95% CI: 0.89 – 0.94). HRS was observed in all of the participants included in the study. The HRS count was significantly higher in the glaucoma group compared to the control group. (average value: 29.65 ± 7.68 and 11.86 ± 5.05, for POAG and healthy subjects, respectively; $P < 0.001$). Of the 65 patients, 42 were using topical prostaglandin (PG) analogs, and no significant difference was observed in the number of HRS between those who were using PG analogs and those who were not ($p = 0.101$). No significant relationship was observed between the duration of glaucoma and the number of HRS ($P = 0.72$).

A positive and high level correlation was found between the average number of HRS and the presence of glaucoma (r = 0.80, $P < 0.001$). A significant positive correlation was found between and the vertical and horizontal cupping diameters (r = 0.45, $P < 0.001$; r = 0.44, $P < 0.001$). Similarly, as cup volume increased, the number of HRS also increased (r = 0.34 $P < 0.001$). A significant negative correlation was observed between the number of HRS and the neuroretinal rim area (r = − 0.46, $P < 0.001$). However, no significant relationship was observed between the number of HRS and the optic disc size ($P = 0.96$). A notable negative correlation was found between the average number of HRS and total RNFL thickness as well as mean GCC thickness (r = − 0.40, $P < 0.001$, r = − 0.41, $P < 0.001$) (Fig. 3). Significant relationship was found between loss volume and the number of HRS, this relationship was stronger in global loss volume (GLV) than in focal loss volume (FLV) (r = 0.41, $P < 0.001$; r = 0.32, $P < 0.001$; Table 2).

After adjusting for age, IOP and SSI, partial correlation coefficients was calculated between the number of HRS and OCT parameters. A positive correlation between the number of HRS and the vertical and horizontal cupping diameters was kept on. (r = 0.45,

Table 1 Demographic and clinical characteristics of the study groups

	Control (Mean ± SD)	Glaucoma (Mean ± SD)	*P*-value
Age (years)	59.75 ± 6.65	62.48 ± 19.77	0.085
Sex (Female / Male)	32 / 33 (49.2%)	27 / 38 (41.5%)	0.378
IOP (mmHg)	14.00 ± 3.46	15.20 ± 4.33	0.610
BCVA (logMAR)	0.00 ± 0.00	0.15 ± 0.35	< 0.001
CCT (μm)	537.11 ± 8.23	532 ± 37.48	0.43
Number of topical antiglaucoma agents	–	2.52 ± 1.20	–
Duration of glaucoma follow-up (months)	–	46.37 ± 52.92	–

Abbreviations: *POAG*: Primary open-angle glaucoma. *IOP*: Intraocular pressure. *BCVA*: Best-corrected visual acuity. *logMAR*: logarithm of the minimum angle of resolution. *CCT*: Central corneal thickness

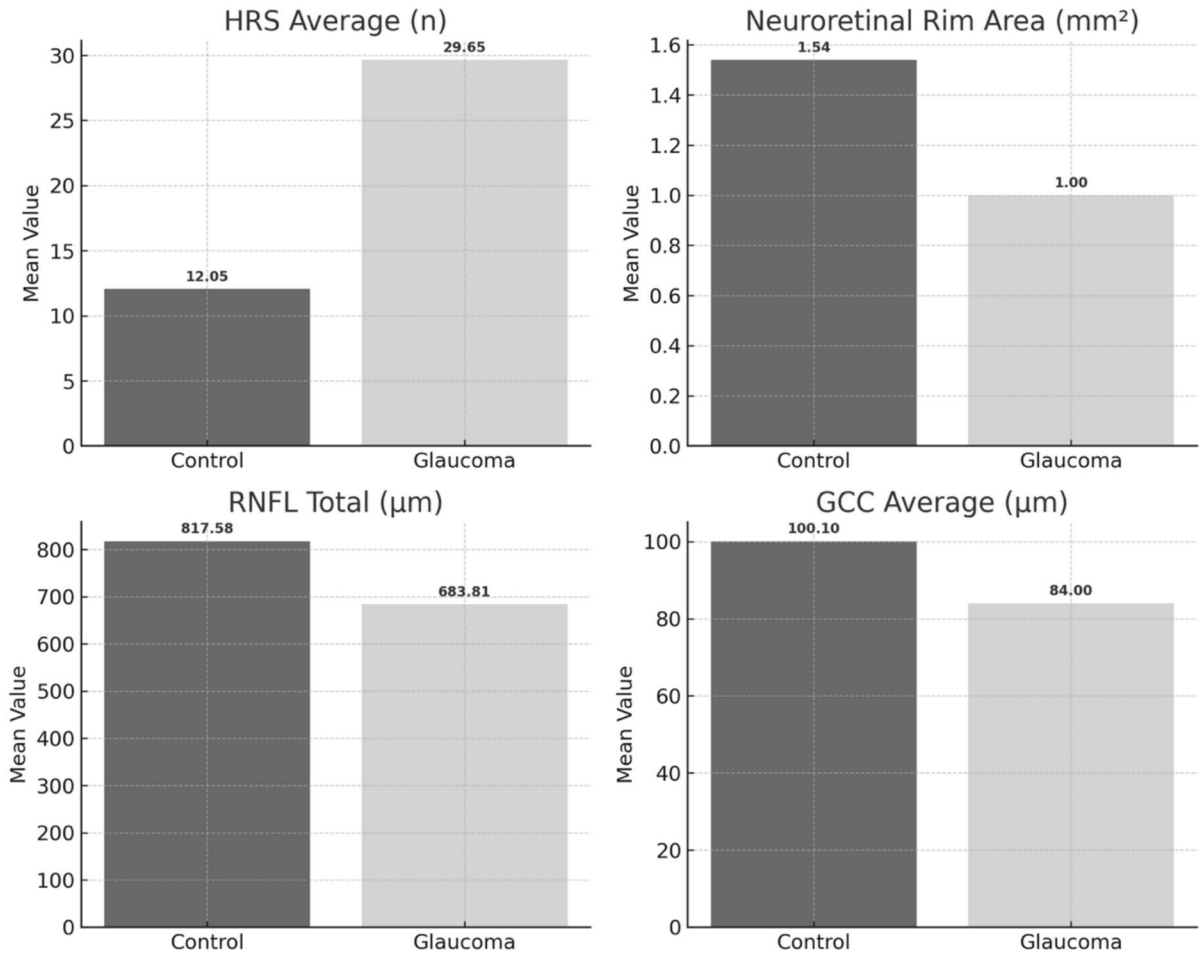

Fig. 2 Bar chart comparing the control and glaucoma groups with respect to average HRS count, neuroretinal rim area, total RNFL thickness, and average GCC thickness. Abbreviations: HRS: Hyperreflective spots. RNFL: Retina nerve fiber layer. GCC: Ganglion cell complex

$P<0.001$; r = 0.45, $P<0.001$). The number of HRS and the neuroretinal rim area was corraleted negatively (r = −0.43, $P<0.001$). Consistently, the correlation between HRS number and total RNFL thickness and mean GCC thickness remained negative. (r = −0.39, $P<0.001$; r = −0.37, $P<0.001$).

Discussion

In the present study, the mean number of HRS was significantly higher in individuals diagnosed with glaucoma compared to the healthy control group. A previous study by Quaranta et al. also reported an increased number of HRS in patients with POAG compared with healthy individuals, and demonstrated that the presence of HRS was significantly correlated with visual field loss [13]. The present study focused on evaluating the relationship between HRS and structural biomarkers obtained from OCT, particularly RNFL and GCC thickness. By demonstrating that HRS is significantly associated with both RNFL and GCC thinning, our results provide novel evidence linking HRS not only to functional impairment but also to structural damage in glaucoma. To the best of our knowledge, this is the first study to describe the correlation between HRS and OCT parameters that reflect the severity of glaucoma.

HRS was originally identified in B-scan OCT images of patients with age-related macular

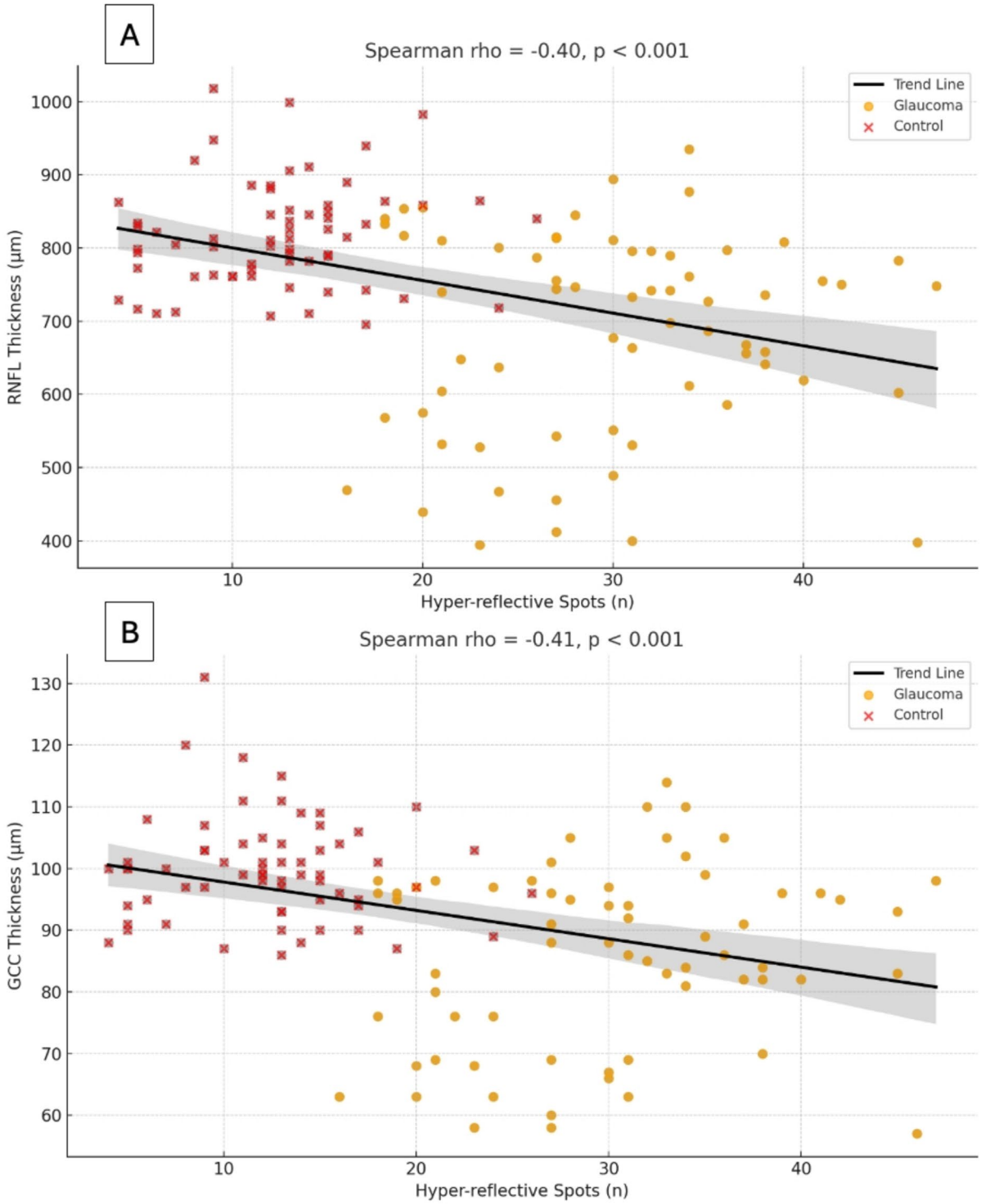

Fig. 3 Scatterplot f HRSs vs. RNFL thickness **A** and GCC thickness **B**. Spearman's rank correlation test. Abbreviations: HRS: Hyperreflective spots. RNFL: Retina nerve fiber layer. GCC: Ganglion cell complex

Table 2 Comparison of SD-OCT parameters of glaucoma and control groups

	Control		Glaucoma		*P*-value
	Mean	SD	Mean	SD	
HRS, Average (n)	12.05	4.89	29.65	7.68	< 0.001
C/D ratio					
Area	0.25	0.15	0.52	0.22	< 0.001
Vertical	0.42	0.20	0.69	0.20	< 0.001
Horizontal	0.51	0.22	0.75	0.17	< 0.001
Neuroretinal rim area (mm^2)	1.54	0.43	1.00	0.46	0.013
Optic disc area (mm^2)	2.09	0.43	2.14	0.42	0.505
Cup volume (mm^3)	0.12	0.18	0.33	0.29	< 0.001
Thickness of RNFL					
Superior (µm)	248.04	25.25	202.53	47.73	< 0.001
Temporal (µm)	151.84	20.34	133.55	26.45	< 0.001
Inferior (µm)	253.46	25.65	206.07	50.63	< 0.001
Nasal (µm)	164.23	25.02	141.64	35.22	< 0.001
Total (µm)	817.58	72.30	683.81	139.40	< 0.001
Thickness of GCC					
Average (mm)	100.1	8.5	84.0	17.04	< 0.001
Superior (mm)	99.42	8.7	86.23	15.31	< 0.001
Inferior (mm)	100.9	8.5	84.91	15.35	< 0.001
FLV (%)	0.68	0.83	5.36	6.05	< 0.001
GLV (%)	2.02	2.22	13.09	12.44	< 0.001

Abbreviations: *HRS*: Hyperreflective spots. *C/D*: Cup to disk. *RNFL*: Retina nerve fiber layer. *GCC*: Ganglion cell complex. *FLV*: Focal loss volume. *GLV*: Global loss volume

degeneration and was suggested to be caused by the aggregation of reactive microglia cells [15]. Various opinions have been raised regarding the content of HRS; one study proposed that they are small intraretinal protein or lipid accumulations that initially precede hard exudates [16]. In another study involving eyes diagnosed with diabetic macular edema, the presence of HRS located in the outer retina was attributed to degenerated photoreceptors or macrophages that phagocytized them [17]. A study analyzing the en face images of OCT angiography suggested that HRS represent lipid-laden macrophages adhered to the vessel walls [18]. Histological examination of human donor eyes with geographic atrophy and acquired vitelliform lesions showed that the HRS visualized in SD-OCT consisted of both migrated retinal pigment epithelium cells and lipid-laden cells corresponding to active microglia [19, 20].

In the treatment of macular edema secondary to branch retinal vein occlusion (BRVO), dexamethasone significantly reduced the number of HRS compared to ranibizumab, highlighting the relationship between HRS and inflammation [21]. In a study conducted on an experimental glaucoma model in rats, it was shown that intravitreal injection of triamcinolone resulted in a decrease in the number of active microglial cells [22]. These results suggest an overlap between the number of HRS and the number of active microglia, indirectly proving the relationship between HRS and neuroinflammation.

Neurodegeneration seen in glaucoma occurs as a result of neuroinflammation involving glial cells and immune system cells in the retina and optic nerve head. Under physiological conditions, microglial cells show small somas and a branched appearance, but when activated, they assume an amoeboid shape with short, thick processes. They gain mobilization, antigen presentation, and phagocytosis capabilities [23]. Microglial functions are controlled by communication between neurons, astrocytes, and Müller cells, and microglial activation is reversible, not leading to secondary neuronal degeneration [7]. However, if the stimulus such as increased IOP continues, inflammation leads to irreversible loss of RGC due to the release of proinflammatory cytokines such as IL-1, TNF alpha, complements and angiogenic factors. In an animal model, the clustering, activation, and migration of microglial cells were detected in

the retina and demyelinated optic nerve head several months before glaucomatous damage developed [24].

In a study conducted using a rat glaucoma model induced by episcleral vein cauterization, hyperreflective opacities were prominently observed at the vitreoretinal interface in the eye with elevated IOP. Histological examination showed that these opacities were primarily composed of clustered active microglial cells. Furthermore, in the same study, retinal microglial cell activation was noted in the control eye, which underwent no intervention, though at a lower intensity [14]. In a mouse model of unilateral laser-induced ocular hypertension, significantly higher numbers of activated microglial cells were observed across all retinal layers in the hypertensive eyes compared to the contralateral normotensive eyes [25]. It was postulated that this activation might result from chronic retinal stress caused by increased IOP, which could lead to microglial activation and subsequent migration to the contralateral eye via the superior colliculus [26].

With the severity of glaucomatous damage, the cup/disc ratio in the OCT examination of the optic nerve head increases both vertically and horizontally, while a proportional thinning of the neuroretinal rim is observed. There is a proportional relationship between the reduction in RNFL thickness in the peripapillary OCT analysis and the decrease in macular GCC thickness, reflecting RGC loss. For these reasons, OCT is frequently used to provide quantitative data for the diagnosis and progression monitoring of glaucoma patients [27]. In this study, a negative correlation was found between the C/D ratio and neuroretinal rim thickness with RNFL and GCC thickness. In our analysis, a positive correlation was found between the average number of HRS and cupping in the optic disc, while a negative correlation was observed with the neuroretinal rim area. As the number of HRS increased, the thinning of RNFL and GCC became significantly pronounced. These data indicate that the number of HRS increases with the progression of glaucomatous damage. This suggests that the number of HRS not only serves as a reliable neuroinflammatory marker in individuals with glaucoma but also reflects the severity of neurodegeneration in direct proportion. Consequently, the number of HRS emerges as an important parameter due to its potential to indicate visual prognosis in glaucoma and its utility in monitoring disease progression.

Limitations of the study include the researcher-dependent nature of the results and the potential for individual variability in assessments. Establishing a standardized method or developing an artificial intelligence-assisted software could reduce the variability of measurements. Glaucoma staging could not be conducted as visual field test results were not available for any patients, and comparison of HRS counts among different stages was thus impracticable. This was considered a limitation that may have weakened the power of the study. Prospective studies including classification of glaucoma based on visual field parameters and investigating the relationship between HRS count could strongly increase the significance of this issue. Axial elongation may result in an underestimation of RNFL and GCC thickness measurements. In our study, the lack of sufficient data to adjust for axial length constitutes one of its limitations.

Additionally, conducting prospective studies with a larger sample size may enhance the reliability of the results and strengthen the establishment of cause-and-effect relationships.

In conclusion, our study demonstrates that HRS can be considered as a novel biomarker to evaluate the severity of glaucoma. Prospective, randomized studies with a larger number of patients are needed to determine the prognostic value of HRS in monitoring glaucomatous progression.

Author contributions Idea: E.K. Study design: E.K., K.K., Data collection: K.K, Y.G. Literature review: K.K., Y.G. Writing the article: K.K., Y.G. Critical review: E.K. Final approval of the version: All authors.

Funding The author(s) received no financial support ort he research, authorship, and/or publication of this article.

Data availability No datasets were generated or analysed during the current study.

Declarations

Conflict of interest The authors report there are no competing interests to declare.

Ethical approval The study was conducted in accordance with the principles of the Helsinki Declaration and received local ethical approval from the Balıkesir University Ethics Committee (2024/238). Written informed consent was obtained from all patients for participation in the study and for the publication of the study results.

References

1. Weinreb RN, Aung T, Medeiros FA (2014) The pathophysiology and treatment of glaucoma. JAMA 311:1901–1911
2. Collaborative Normal-Tension Glaucoma Study Group (1998) The effectiveness of intraocular pressure reduction in the treatment of normal-tension glaucoma. Am J Ophthalmol 126:498–505
3. Fernández-Albarral JA, Ramírez AI, de Hoz R, Matamoros JA, Salobrar-García E, Elvira-Hurtado L et al (2024) Glaucoma: from pathogenic mechanisms to retinal glial cell response to damage. Front Cell Neurosci 18:1–26
4. Tezel G (2013) Immune regulation toward immunomodulation for neuroprotection in glaucoma. Curr Opin Pharmacol 13:23–31
5. Vecino E, Rodriguez FD, Ruzafa N, Pereiro X, Sharma SC (2016) Glia–neuron interactions in the mammalian retina. Prog Retin Eye Res 51:1–40
6. Barron KD (1995) The microglial cell: a historical review. J Neurol Sci 134:57–68
7. Nakamura Y (2002) Regulating factors for microglial activation. Biol Pharm Bull 25:945–953
8. Curcio CA, Allen KA (1990) Topography of ganglion cells in human retina. J Comp Neurol 300:5–25
9. Vujosevic S, Bini S, Torresin T, Casciano M, Cavarzeran F, Midena E (2017) Hyperreflective retinal spots in normal and diabetic eyes. Retina 37:1092–1103
10. Framme C, Schweizer P, Imesch M, Wolf S, Wolf-Schnurrbusch U (2012) Behavior of SD-OCT–detected hyperreflective foci in the retina of anti-VEGF–treated patients with diabetic macular edema. Invest Ophthalmol Vis Sci 53:5814–5818
11. Coscas G, De Benedetto U, Coscas F, Li Calzi CI, Vismara S, Roudot-Thoraval F et al (2013) Hyperreflective dots: a new spectral-domain optical coherence tomography entity for follow-up and prognosis in exudative age-related macular degeneration. Ophthalmologica 229:32–37
12. Pilotto E, Miante S, Torresin T, Puthenparampil M, Frizziero L, Federle L et al (2020) Hyperreflective foci in the retina of active relapse-onset multiple sclerosis. Ophthalmology 127:1774–1776
13. Quaranta L, Bruttini C, De Angelis G, Montescani S, Ardizzone A, Katsanos A et al (2021) A comparison of hyperreflective retinal spot counts in optical coherence tomography images from glaucomatous and healthy eyes. J Clin Med 10:4668
14. Rodrigo MJ, Subías M, Montolío A, Méndez-Martínez S et al (2021) Analysis of parainflammation in chronic glaucoma using vitreous-OCT imaging. Biomedicines 29:1792
15. Coscas G, Coscas F, Vismara S, Zourdani A, Calzi CI (2009) Optical coherence tomography in age-related macular degeneration, 1st edn. Springer, Berlin
16. Bolz M, Schmidt-Erfurth U, Deak G, Mylonas G, Kriechbaum K, Scholda C (2009) Optical coherence tomographic hyperreflective foci: a morphologic sign of lipid extravasation in diabetic macular edema. Ophthalmology 116:914–920
17. Uji A, Murakami T, Nishijima K, Akagi T, Horii T, Arakawa N et al (2012) Association between hyperreflective foci in the outer retina, status of photoreceptor layer, and visual acuity in diabetic macular edema. Am J Ophthalmol 153:710–717
18. Murakami T, Suzuma K, Dodo Y, Yoshitake T, Yasukura S, Nakanishi H et al (2018) Decorrelation signal of diabetic hyperreflective foci on optical coherence tomography angiography. Sci Rep 8:8798
19. Cao D, Leong B, Messinger JD, Kar D, Ach T, Yannuzzi LA et al (2021) Hyperreflective foci, optical coherence tomography progression indicators in age-related macular degeneration, include transdifferentiated retinal pigment epithelium. Invest Ophthalmol Vis Sci 62:34
20. Chen KC, Jung JJ, Curcio CA, Balaratnasingam C, Gallego-Pinazo R, Dolz-Marco R et al (2016) Intraretinal hyperreflective foci in acquired vitelliform lesions of the macula: clinical and histologic study. Am J Ophthalmol 164:89–98
21. Karalezli A, Kaderli ST, Kaderli A, Kaya C, Sul S (2023) Comparison of changes in number of hyperreflective dots after intravitreal ranibizumab or dexamethasone implant in patients with branch retinal vein occlusion. Taiwan J Ophthalmol 14:387–393
22. Singhal S, Lawrence JM, Salt TE, Khaw PT, Limb GA (2010) Triamcinolone attenuates macrophage/microglia accumulation associated with NMDA-induced RGC death and facilitates survival of Müller stem cell grafts. Exp Eye Res 90:308–315
23. Beynon SB, Walker FR (2012) Microglial activation in the injured and healthy brain: What are we really talking about? Practical and theoretical issues associated with the measurement of changes in microglial morphology. Neuroscience 225:162–171
24. Bosco A, Steele MR, Vetter ML (2011) Early microglia activation in a mouse model of chronic glaucoma. J Comp Neurol 519:599–620
25. Ramírez AI, de Hoz R, Fernández-Albarral JA, Salobrar-Garcia E, Rojas B et al (2020) Time course of bilateral microglial activation in a mouse model of laser-induced glaucoma. Sci Rep 10:4890
26. Sapienza A, Raveu AL, Reboussin E et al (2016) Bilateral neuroinflammatory processes in visual pathways induced by unilateral ocular hypertension in the rat. J Neuroinflammation 20(13):44
27. Geevarghese A, Wollstein G, Ishikawa H, Schuman JS (2021) Optical coherence tomography and glaucoma. Annu Rev Vis Sci 7:693–726